RESULTS AND DISCUSSION

CHAPTER IV

RESULTS AND DISCUSSION

This chapter details the results of the study on accelerated aging of cocoa mucilage wine through hydrodynamic and standardisation of the process parameters. Three replications were performed for all the analysis. Data is represented in the form of average of replications with standard deviation as graphs or tables. This section includes the evaluation and examination of the outcomes of experiments.

4.1 PHYSICO-CHEMICAL CHARACTERISTICS OF COCOA MUCILAGE

Fresh cocoa mucilage or drippings were hygienically collected from cocoa beans as described in section 3.2 for the purpose of conducting the study. Various quality parameters of the cocoa mucilage were analysed and the results are shown in the Table 4.1.

Table 4.1 Physico-chemical characteristics of cocoa mucilage

Quality parameters	Result
Total phenolic content	107.03 mgGAE/ml
Total soluble solids	17.7°Brix
Ph	3.97
Titrable acidity	0.3 g/ml (tartaric acid)
Vitamin C	1.01 mg/100ml
Antioxidant scavenging activity (DPPH)	34.3%
Reducing sugar	10.41%
Color	
L*	72.25
a*	2.00
b*	9.3

The placenta, mucilaginous pulp and cocoa beans make up the cocoa pod. The mucilaginous pulp envelops the cocoa bean. It was observed that the total phenolic content of the pulp was 107.03 mgGAE/ml. 17.7°Brix was the TSS value that had been

identified. pH of the pulp was 3.97, which is acidic. It was observed that the mucilage had a titrable acidity of 0.3g/ml. The concentration of ascorbic acid (vitamin C) was found to be 1.01 mg/100 ml. The value for antioxidants in terms of DPPH scavenging activity was 34.3%. In color analysis, the L*, a* and b* values of the pulp were calculated as 72.25, 2.00 and 9.3 respectively. The pulp had about 10.41% reducing sugars.

4.2 PHYSICO-CHEMICAL CHARACTERISTICS OF WINE PREPARED FROM COCOA MUCILAGE

The total phenolic content of the wine was measured at 258 mg GAE/mL, significantly higher than the TPC of the pulp, which was 107.03 mg GAE/ml. Several processes contribute to the phenolic transformations in wine during and after production. These include anthocyanin degradation, tannin interactions with proteins and polysaccharides, procyanidin cation formation, oxidation and polymerization reactions of procyanidins, anthocyanin copigments synthesis, reactions of anthocyanins with compounds containing polarized double bonds and condensation reactions between anthocyanins and tannins (Hatice & Ezgi, 2017).

The TSS content of prepared wine is 21.5°Brix which is higher compared to TSS of mucilage (17.7°Brix). TSS was increased in the wine because sucrose solution was added for the purpose of fermentation which provided the medium for activation of yeast.

Plate 4.1 Cocoa mucilage wine

The pH of prepared wine was obtained as 3.66 which is slightly lower than the pH of mucilage (3.97). The preferred wine pH is around 3.6 and the better pH for yeast and lactic acid bacteria is around 4.5. However, spoilage bacteria can also grow well at

pH 4.5. But spoilage bacteria do not grow well below pH 3.6. Wine yeasts and some lactic acid bacteria can still metabolize in a pH range of 3.3–3.6. The low pH can prolong the fermentation process due to slow growth of microorganisms involved (Jacobson, 2006).

The titrable acidity of wine was found to be 0.0381 g/ml, which is lower than the value for mucilage (0.3 g/ml). Throughout the fermentation process, no consistent pattern in the change in titrable acidity was observed. However, it was found that the titratable acidity of the must had reduced by the end of fermentation (Kasture and Kadam, 2018).

The vitamin C value for wine was obtained as 0.016 mg/100 ml. This is lower compared to vitamin C content of mucilage (1.01 mg/100 ml). All wine varieties showed a drop in L-ascorbic acid level following the conclusion of the fermentation process. Other publications claim that several percent of L-ascorbic acid were lost during the alcoholic fermentation process (Czyżowska *et al*., 2015). The loss of L-ascorbic acid could have been caused by a number of circumstances.

The antioxidant scavenging activity (DPPH) of wine showed a higher value (41.72%) compared to that of cocoa mucilage (34.3%). Red wines exhibit stronger antioxidant activity. Polymeric phenolic compounds are responsible for half of the total scavenging radical activity of red wine (as measured by the DPPH and ABTS techniques). The order of reactivity for the remaining 50% is as follows: phenolic acids and flavanols are the next most active, followed by anthocyanins and flavan-3-ol. (Fernandez *et al*., 2004).

The reducing sugar content was determined to be 21.42%, indicating an increase compared to the 10.41% observed in mucilage. The typicality of the cultivars and the winery's winemaking process are closely related to the higher reducing sugar concentration of wine. Additionally, the fluctuation in reducing sugar content and other physicochemical qualities is influenced by other factors such soil type, grape sanitary conditions, climate, weather and wine management (Neto *et al*., 2015)

The cocoa mucilage wine had colour characteristics: L* value of 68.25, a* value of 2.02 and b* value of 11.03. Higher L* value indicates lighter colour of mucilage. The

alcohol content of prepared wine was measured to be 7%. It was observed that alcohol generally had a greater impact on taste and mouthfeel characteristics than fragrance descriptors. (King *et al*., 2013).

Table 4.2 Physico-chemical characteristics of freshly prepared cocoa mucilage wine

Quality parameters	Result
Total phenolic content	258 mgGAE/ml
Total soluble solids	21.5°Brix
Ph	3.66
Titrable acidity	0.0381 g/ml (tartaric acid)
Vitamin C	0.016 mg/100ml
Antioxidant scavenging activity (DPPH)	41.72%
Reducing sugar	21.42%
Alcohol content	7%
Color L* a* b*	 68.25 2.02 11.03
Minerals Calcium Potassium Magnesium Phosphorous	 171 mg/ml 950 mg/ml 82.5 mg/ml 62.47 mg/ml

4.3 DEVELOPMENT OF HYDRODYNAMIC CAVITATION REACTOR SYSTEM

A hydrodynamic cavitation reactor system with a 10 litres capacity was developed to accelerate the ageing process of cocoa mucilage wine. The system includes a storage tank, a 1.5hp pump, various cavitation elements with different geometries, a digital flow meter, pressure gauges and a piping assembly, as outlined in Section 3.6.

Its operation relies on the cavitation effect, which is induced in the fluid flowing through a closed pipe at varying operating pressures.

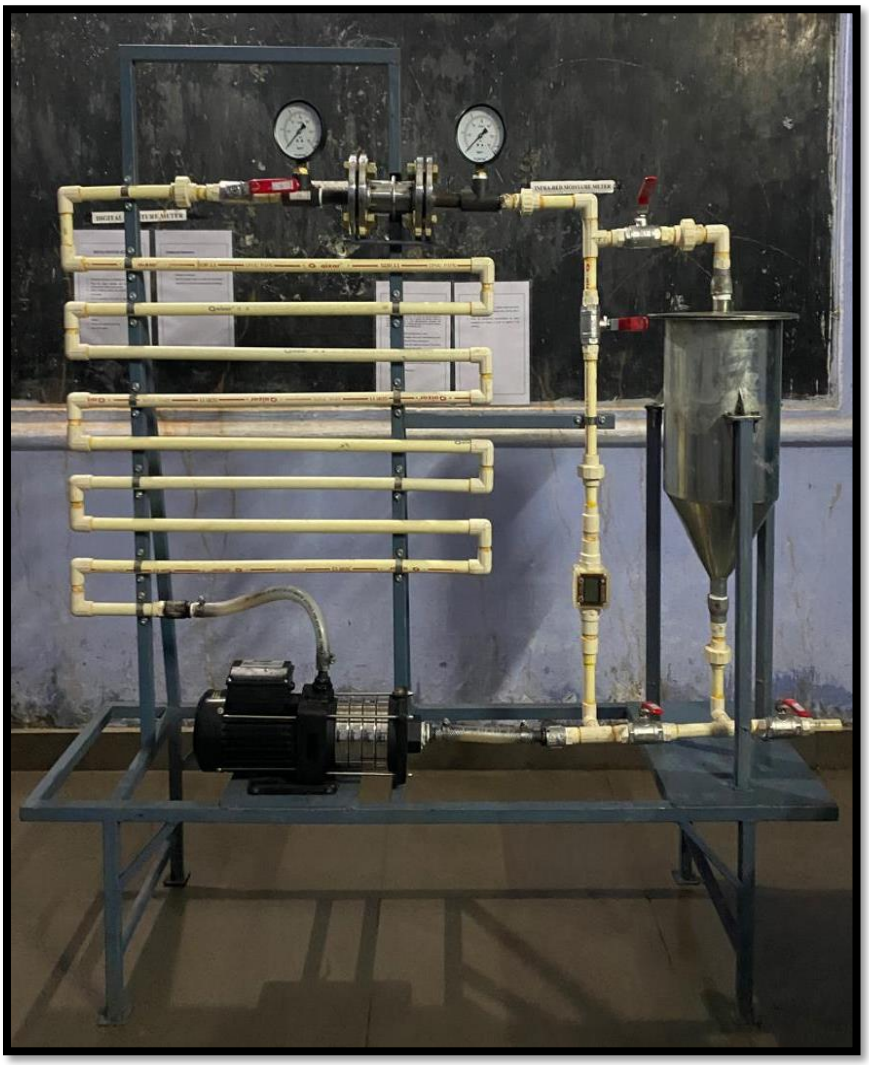

Plate 4.2 Hydrodynamic cavitation reactor system

4.4 OPTIMISATION OF PROCESS PARAMETERS OF HYDRODYNAMIC CAVITATION REACTOR

The process conditions were optimized to achieve maximum volume flow rate, energy release and total phenolic content. Table 4.3 presents the influence of independent parameters of hydrodynamic cavitation (HC) treatments on the response variables, including cavitation number, volume flow rate, total phenolic content and energy released.

Table 4.3 Effect of process parameters on the performance of HC reactor system for the accelerated ageing of cocoa mucilage wine

Runs	Process pressure (Bar)	Time of flow (Min)	Type of element	Cavitation Number	Volume Flow Rate (L/h)	Total Phenolic Content (mgGAE/ml)	Energy released (J/ml)
1	3	30	Orifice	0.039	15.9	308	4.77
2	4	30	Orifice	0.0092	6.5	307.8	1.3
3	3	60	Orifice	0.041	16.1	310	7.084
4	4	60	Orifice	0.0097	6.7	310.14	2.948
5	2.79289	45	Orifice	0.045	17.9	308.9	7.86418
6	4.20711	45	Orifice	0.007	5.5	308.78	1.70863
7	3.5	23.7868	Orifice	0.021	10.7	309.41	2.29067
8	3.5	66.2132	Orifice	0.031	13	312.4	7.1731
9	3.5	45	Orifice	0.028	12.1	312.8	3.993
10	3.5	45	Orifice	0.029	12.5	312.88	4.6875
11	3.5	45	Orifice	0.03	12.8	313.87	5.184
12	3.5	45	Orifice	0.029	12.4	313.74	4.65
13	3.5	45	Orifice	0.027	12.2	312.41	5.49
14	3	30	Slit venturi	0.413	22	317.89	6.6
15	4	30	Slit venturi	0.1	9.1	317.57	1.82
16	3	60	Slit venturi	0.85	23.5	318.43	10.34
17	4	60	Slit venturi	0.104	9.3	318	4.092

18	2.79289	45	Slit venturi	0.465	24.3	317	10.676
19	4.20711	45	Slit venturi	0.0818	8	317.92	2.48528
20	3.5	23.7868	Slit venturi	0.221	14.7	318.44	3.14699
21	3.5	66.2132	Slit venturi	0.232	15	321.01	8.27665
22	3.5	45	Slit venturi	0.33	17.8	321	6.56
23	3.5	45	Slit venturi	0.316	17.5	321.54	6.5625
24	3.5	45	Slit venturi	0.304	17.2	321.87	6.966
25	3.5	45	Slit venturi	0.312	17.4	321.57	6.97
26	3.5	45	Slit venturi	0.322	17.8	320.14	8.01
27	3	30	Elliptical venturi	0.662	11	310	3.3
28	4	30	Elliptical venturi	0.9814	4	312	0.8
29	3	60	Elliptical venturi	0.771	11.7	313.54	5.148
30	4	60	Elliptical venturi	0.14	4.4	313.44	1.936
31	2.79289	45	Elliptical venturi	0.989	14	310.11	6.15076
32	4.20711	45	Elliptical venturi	0.1	3.5	310.01	1.08731
33	3.5	23.7868	Elliptical venturi	0.221	5.8	311.85	1.24167
34	3.5	66.2132	Elliptical venturi	0.392	7.7	314.14	4.24868
35	3.5	45	Elliptical venturi	0.327	7	315.47	2.31
36	3.5	45	Elliptical venturi	0.315	6.9	315.81	2.5875
37	3.5	45	Elliptical venturi	0.332	7.1	315.05	2.8755
38	3.5	45	Elliptical venturi	0.324	7	315.09	2.625
39	3.5	45	Elliptical venturi	0.312	6.9	315.077	3.105

4.4.1 Effect of process pressure, time of flow and type of cavitation element on total phenolic content

The effects of process pressure, time of flow and type of cavitation element on the total phenolic content of cocoa mucilage wine are presented in Table 4.3. The TPC ranged from 307.8 to 321.87 mg GAE/mL, with the highest value observed at a process pressure of 3.5 bar and a flow time of 45 minutes using the slit venturi treatment. A strong correlation was observed between process pressure, time of flow and the type of cavitation element, indicating their significant influence on the TPC of the wine.

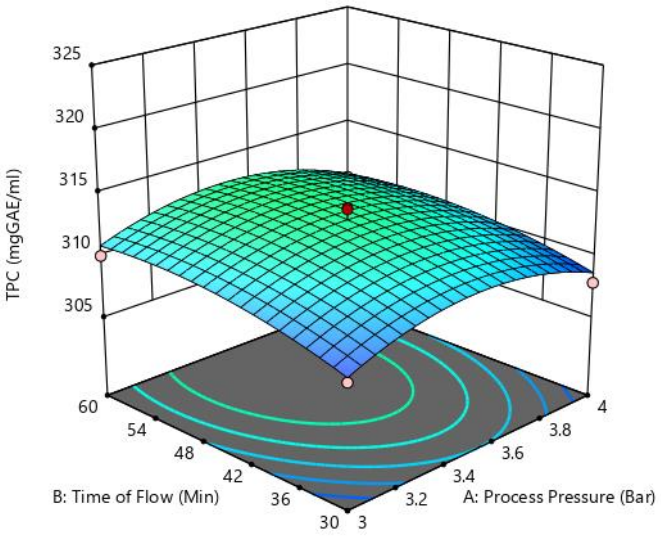

a

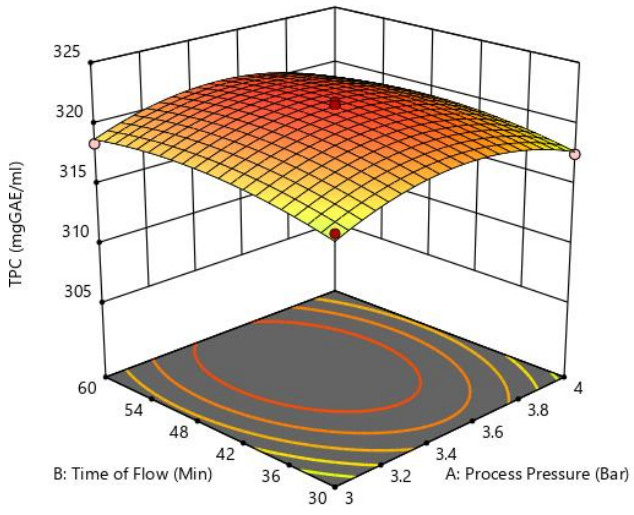

b

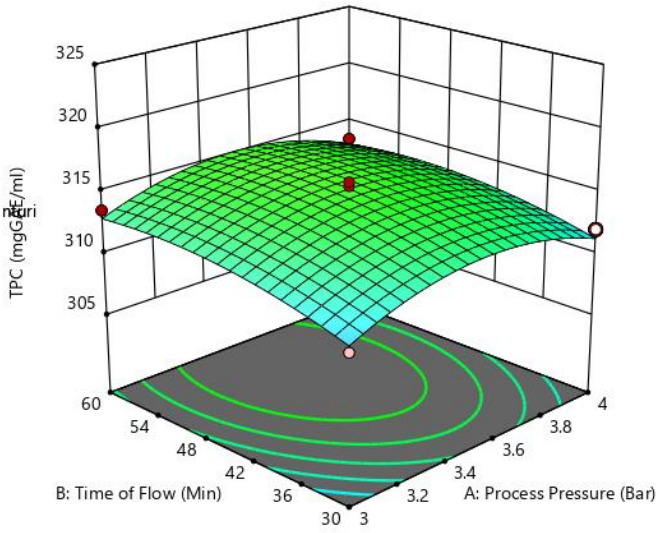

c

Fig. 4.1 Surface response on total phenolic content on various cavitation elements (a) Orifice (b) Slit venturi (c) elliptical venturi

The response surface plot (Fig. 4.1) clearly demonstrates that the effects of process pressure and flow time on the total phenolic content of wine follow a similar trend across all three cavitation elements. As shown in Fig. 4.1, the TPC initially increases significantly with rising process pressure and time of flow, but further increases in these parameters lead to a notable decline in TPC values. In Fig. 4.1(a), the TPC of wine treated using the slit venturi ranged from 317 to 321.87 mg GAE/mL, with the highest value achieved at 45 minutes and 3.5 bar. Similar trends are observed in Fig. 4.1(b) and Fig. 4.1(c), with maximum TPC values of 315.81 mg GAE/mL and 313.87 mg GAE/mL respectively, under the same operating conditions.

The variation in TPC during HC treatment is attributed to the release of phenolic compounds from the cells, facilitated by the coalescence caused by the cavitation effect. Recent studies indicate that phenolic compounds are bound to carbohydrates, proteins, lignin and pectin. The ability of HC to break down larger molecules into simpler ones results in the release of these phenolic compounds into the medium (Albanese *et al*., 2019). Additionally, phenolic compounds have been found to remain stable and resistant to degradation during various HC treatment durations. For instance, Gani *et al*., (2016) observed a significant increase in TPC from 1.39 to 1.50 mgGAE/100 g, when

strawberry juice was subjected to ultrasound treatment for 0–40 minutes, followed by a decline at 60 minutes.

The ANOVA results (Table 4.4) indicate that the fitted quadratic model is highly significant, with a p-value of less than 0.0001. The high coefficient of determination (R^2 = 0.9822) confirms that the model provides an excellent fit.

Table 4.4 Analysis of variance (ANOVA) for TPC of cocoa mucilage wine

Source	Sum of Squares	df	Mean Square	F-value	p-value	
Model	651.01	11	59.18	135.51	< 0.0001	
A-Process Pressure	0.1803	1	0.1803	0.4127	0.526	
B-Time of Flow	19.07	1	19.07	43.66	< 0.0001	
C-Type of Element	508.51	2	254.25	582.17	< 0.0001	
AB	0.2914	1	0.2914	0.6672	0.4212	
AC	0.2509	2	0.1254	0.2872	0.7526	
BC	1.2	2	0.602	1.38	0.2691	significant
A^2	108.78	1	108.78	249.08	< 0.0001	
B^2	23.99	1	23.99	54.94	< 0.0001	
Residual	11.79	27	0.4367			
Lack of Fit	7.88	15	0.525	1.61	0.206	
Pure Error	3.92	12	0.3264			
Cor Total	662.8	38				

The polynomial equation (Eq. 4.1) predicts the total phenolic content by accounting for the linear, interaction and quadratic effects of process pressure (A) and time of flow (B).

$$Total\ phenolic\ content\ (Slit\ venturi) = 194.48 + 64.99A + 0.54B - 0.021AB - 9.13A^2 - 0.005B^2 \quad (4.1a)$$

$$Total\ phenolic\ content\ (Orifice) = 185.12 + 64.80A + 0.57B - 0.021AB - 9.13A^2 - 0.005B^2 \quad (4.1b)$$

$$Total\ phenolic\ content\ (Elliptical\ venturi) = 185.85 + 65.30A + 0.57B - 0.021AB - 9.13A^2 - 0.005B^2 \quad (4.1c)$$

The positive coefficients for 'A' and 'B' indicate that an increase in process pressure (A) and time of flow (B) leads to a rise in TPC. The negative coefficient for AB suggests that the interaction between process pressure (A) and flow time (B) has a detrimental effect on TPC. In other words, changes in one variable can affect the influence of the other on TPC.

4.4.2 Effect of process pressure, time of flow and type of cavitation element on cavitation number

The effect of process pressure, time of flow and type of cavitation element on the cavitation number is presented in Table 4.3. The cavitation number ranged from 0.007 to 0.989. The relationship between process pressure, flow time and cavitation element type showed a strong correlation with the cavitation number.

The response surface plot (Fig. 4.2) clearly illustrates that the effects of process pressure and time of flow on the cavitation number exhibit a similar trend across all three cavitation elements. As shown in Fig. 4.2, the cavitation number is significantly ideal for the treatments conducted in the slit venturi compared to those in the orifice and elliptical venturi.

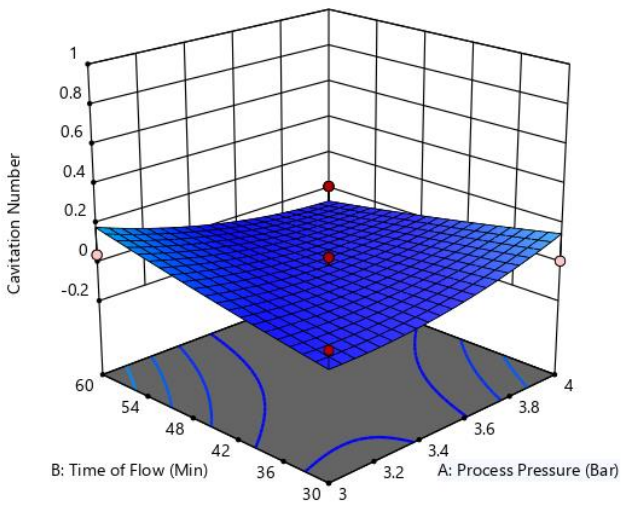

a

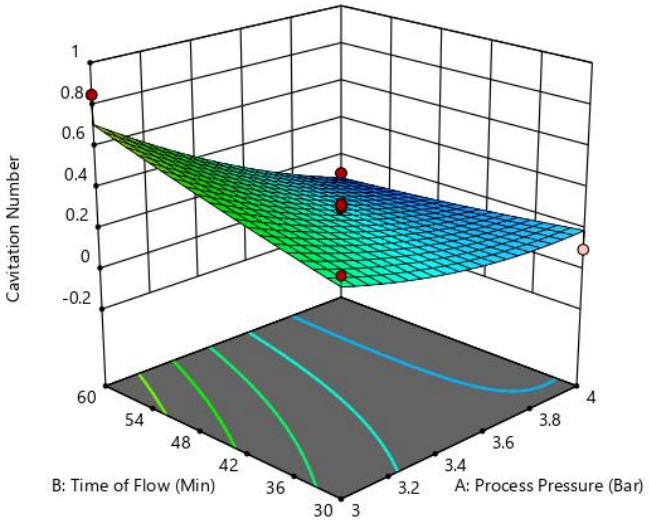

b

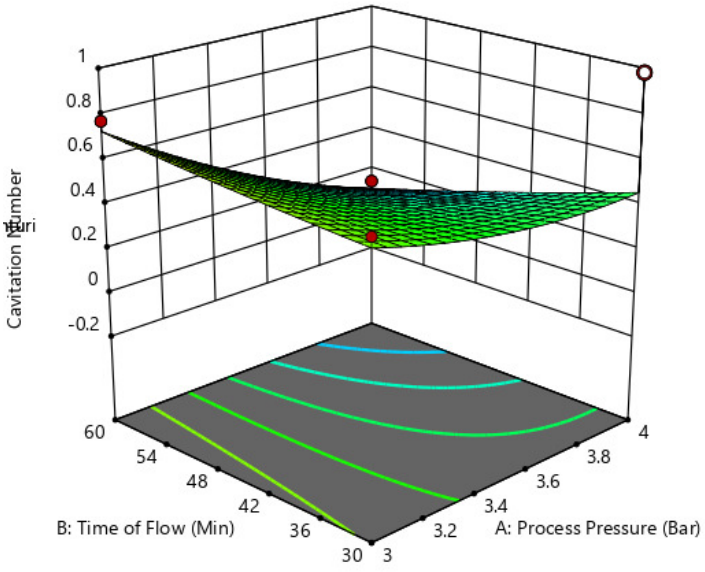

c

Fig. 4.2 Surface response on cavitation number on various cavitation elements (a) Orifice (b) Slit venturi (c) elliptical venture

Ideally, cavitation initiation occurs at a cavitation number of 1. However, a lower cavitation number has been observed depending on the size of the cavitation element and variations in inlet pressure. According to Saharan *et al*., (2013), the ideal cavitation number ranges from 0.15 to 0.4, depending on the geometry of the

constriction. However, a decrease in the cavitation number below the ideal range can lead to choked cavitation (Saharan et al., 2011). Therefore, the current study has reduced the cavitation number to a level where cavitation can occur without adversely affecting the wine's properties, demonstrating a more effective cavitation impact on wine aging.

The polynomial equation (Eq. 4.2) predicts the cavitation number by considering the linear, interaction, and quadratic effects of process pressure (A) and time of flow (B).

Table 4.5 Analysis of variance (ANOVA) for cavitation number

Source	Sum of Squares	df	Mean Square	F-value	p-value	
Model	2.13	11	0.1937	8.1	< 0.0001	significant
A-Process Pressure	0.4495	1	0.4495	18.8	0.0002	
B-Time of Flow	0	1	0	0.0005	0.9819	
C-Type of Element	1.22	2	0.609	25.47	< 0.0001	
AB	0.1598	1	0.1598	6.68	0.0154	
AC	0.1801	2	0.0901	3.77	0.0361	
BC	0.0562	2	0.0281	1.17	0.3243	
A^2	0.0673	1	0.0673	2.82	0.1049	
B^2	0.0018	1	0.0018	0.0758	0.7852	
Residual	0.6456	27	0.0239			
Lack of Fit	0.6449	15	0.043	767.74	< 0.0001	
Pure Error	0.0007	12	0.0001			
Cor Total	2.78	38				

The ANOVA results (Table 4.5) show that the fitted quadratic model is highly significant, with a p-value below 0.0001. The high coefficient of determination (R^2 = 0.9822) further confirms that the model provides an excellent fit.

$$Cavitation\ Number\ (Slit\ venturi) = 1.94 - 1.30A + 0.053B - 0.015AB + 0.23A^2 + 0.00004B^2 \quad (4.2a)$$

$$Cavitation\ Number\ (Orifice) = 0.52 - 0.93A + 0.050B - 0.015AB + 0.23A^2 + 0.00004B^2 \quad (4.2b)$$

$$Cavitation\ Number\ 9Elliptical\ venturi) = 2.41 - 1.30A + 0.047B - 0.015AB + 0.23A^2 + 0.00004B^2 \quad (4.2c)$$

The negative coefficient for 'A' indicates that an increase in process pressure (A) reduces the cavitation number, while the positive coefficient for 'B' shows that a longer flow time (B) results in a higher cavitation number. The negative coefficient for AB suggests that the interaction between process pressure (A) and flow time (B) negatively impacts the cavitation number. In other words, changes in one variable can alter the effect of the other on the cavitation number.

4.4.3 Effect of process pressure, time of flow and type of cavitation element on volume flow rate

The effect of process pressure, time of flow and type of cavitation element on the volume flow rate is presented in Table 4.3. The maximum volume flow rate (VFR) was achieved at a process pressure of 2.79 bar and a flow time of 45 minutes, using the slit venturi treatment. The relationship between process pressure, time of flow and cavitation element type showed a strong correlation with the volume flow rate.

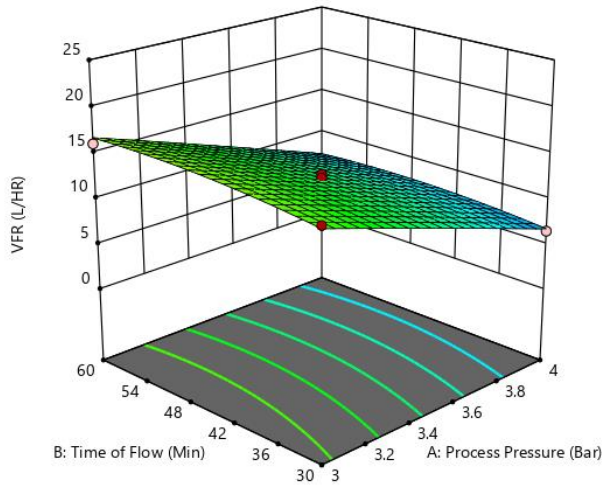

a

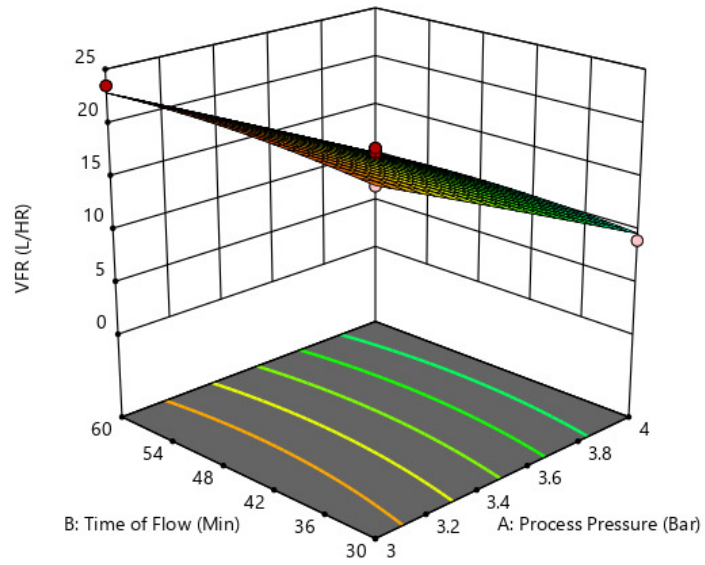

b

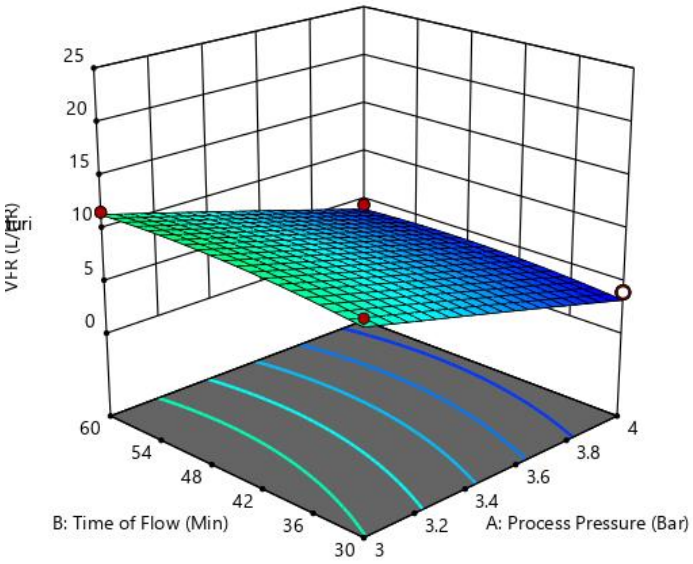

c

Fig. 4.3 Surface response on volume flow rate on various cavitation elements (a) Orifice (b) Slit venturi (c) elliptical venturi

The response surface plot (Fig. 4.3) clearly shows that the effect of process pressure and time of flow on the volume flow rate (VFR) follows a similar trend across all three cavitation elements. Fig. 4.3 illustrates that the VFR reaches its highest value at the initial process parameters, but a further decrease in pressure leads to a significant reduction in VFR. From Fig. 4.3(a), 4.3(b), and 4.3(c), it is evident that the VFR exhibits

a similar trend with respect to process parameters such as pressure and time. Additionally, the slit venturi element shows the highest VFR, as its geometry, particularly the constriction area, has a direct relationship with the volume flow rate.

The ANOVA results (Table 4.6) indicate that the fitted quadratic model is highly significant, with a p-value of less than 0.0001. The high coefficient of determination (R^2 = 0.9838) confirms that the model provides the best fit.

Table 4.6 Analysis of variance (ANOVA) for volume flow rate

Source	Sum of Squares	df	Mean Square	F-value	p-value	
Model	1119.79	11	101.8	148.59	< 0.0001	significant
A-Process Pressure	557.16	1	557.16	813.29	< 0.0001	
B-Time of Flow	3.81	1	3.81	5.56	0.0258	
C-Type of Element	522.96	2	261.48	381.68	< 0.0001	
AB	0.2133	1	0.2133	0.3114	0.5814	
AC	28.48	2	14.24	20.79	< 0.0001	
BC	0.2133	2	0.1066	0.1557	0.8566	
A^2	0.0548	1	0.0548	0.08	0.7794	
B^2	6.93	1	6.93	10.12	0.0037	
Residual	18.5	27	0.6851			
Lack of Fit	17.9	15	1.19	23.86	< 0.0001	
Pure Error	0.6	12	0.05			
Cor Total	1138.28	38				

The individual components and their interactions are represented by the estimated coefficients of the quadratic term, which predicts the volume flow rate. This polynomial equation accounts for both the linear and quadratic relationships between process pressure (A), time of flow (B) and VFR, as well as the interaction between process pressure (A) and flow time (B). Positive and negative terms predict synergistic and antagonistic effects respectively. The linear term ‘A’, being negative, indicates that an increase in process pressure leads to a decrease in VFR and vice versa. Similarly, the

positive linear term ‘B’ suggests that an increase in time of flow results in an increase in VFR. The interaction term ‘AB’ indicates that the combination of process pressure and time of flow negatively impacts VFR. The quadratic terms A^2 and B^2, suggest that the relationship between process pressure, time of flow and VFR is not purely linear but may involve a quadratic component, which, in this case, has a negative effect.

$$Volume\ Flow\ Rate\ (Slit\ venturi) = 49.40554 - 10.30A + 0.314B - 0.018AB - 0.21A^2 - 0.003B^2 \quad (4.3a)$$

$$Volume\ Flow\ Rate\ (Orifice) = 32.18 - 6.85A + 0.32B - 0.018AB - 0.21A^2 - 0.003B^2 \quad (4.3b)$$

$$Volume\ Flow\ Rate\ (Elliptical\ venturi) = 21.44 - 5.05A + 0.32B - 0.018AB - 0.21A^2 - 0.003B^2 \quad (4.3c)$$

4.4.4 Effect of process pressure, time of flow and type of cavitation element on energy released

The values of energy released during HC treatment are presented in Table 4.3. The impact of process pressure, time of flow and type of cavitation element on the energy released is illustrated in Fig. 4.4. The maximum energy release was achieved at a process pressure of 2.79 bar and a flow time of 45 minutes, with the slit venturi treatment yielding this result.

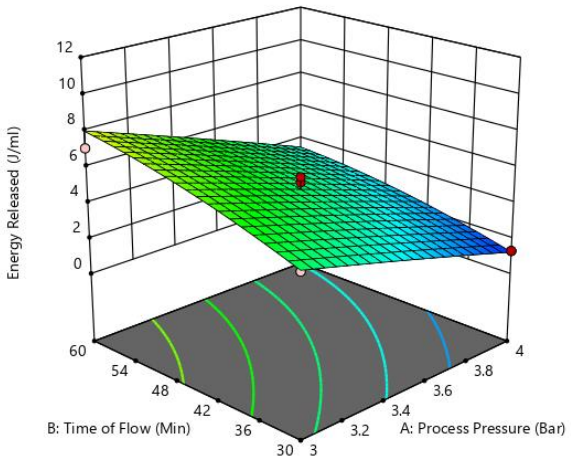

a

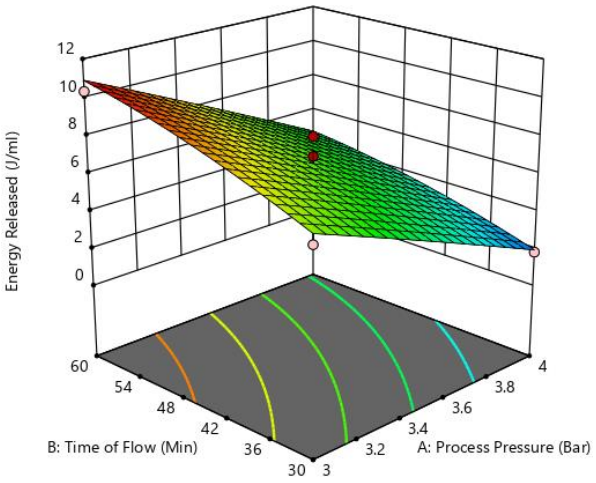

b

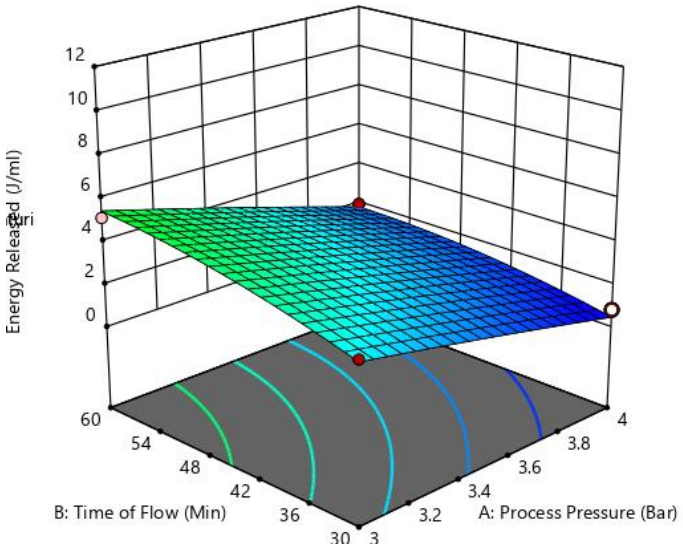

c

Fig. 4.4 Surface response on energy released on various cavitation elements (a) Orifice (b) Slit venturi (c) elliptical venturi

The response surface plot (Fig. 4.4) clearly shows that the effect of process pressure and time of flow on the energy released follows a similar trend across all three cavitation elements. Fig. 4.4 illustrates that energy release increases with time of flow and vice versa, while a decrease in pressure also results in higher energy release. From Fig. 4.4(a), 4.4(b) and 4.4(c), it is evident that the energy released exhibits a similar

trend with respect to process parameters such as pressure and time. Additionally, the slit venturi element shows the highest energy release, as it has a direct relationship with both the volume flow rate and time of flow.

This is because during the collapse of cavities, hydrodynamic cavitation releases a significant amount of energy over a very small area, creating "hot spots" that result in high energy densities due to the extremely high temperatures and pressures developed in localized regions (Hilares *et al*., 2017). Studies on beer brewing have shown that HC-assisted brewing consumes less overall specific energy than conventional brewing, with energy savings of up to 13% (Albanese *et al*., 2017). Nakashima *et al*., (2016) found that HC treatment of corn stover (2.24×10^5 g glucose/J) was more efficient than ultrasound treatment (0.11×10^5 g glucose/J). Therefore, it can be inferred that HC is a promising technology that can be effectively applied in the aging process of cocoa mucilage wine.

From the ANOVA (Table 4.7), the quadratic model is found to be the best fit with p-value less than 0.0001 and R^2 value of 0.9596.

The individual components and their interactions were revealed by the estimated coefficients of the quadratic term, which predicts the value of energy released. This polynomial equation models the energy released in J/ml as a function of process pressure (A) and time of flow (B), considering linear, interaction and quadratic effects. Furthermore, the positive and negative terms indicated synergistic and antagonistic effects. The ‘A’ and ‘B’ terms represents the linear effects of process pressure (A) and time of flow (B) on energy released in all the cavitation reactors. The negative coefficient revealed that increasing process pressure decreases the energy released during cavitation. Also, the positive coefficient indicates that the increase in time of flow will increase the energy released during the treatment. The combination term ‘AB’ suggests that the combination of process pressure and time has a negative impact on energy released as that in same case of VFR. Similarly, quadratic terms A^2 and B^2 suggests that the relationship between process pressure and time of flow with energy released is not strictly linear but may have a quadratic component but, in this case, it has a negative effect.

Table 4.7 Analysis of variance (ANOVA) for energy released during HC treatment

Source	Sum of Squares	Df	Mean Square	F-value	p-value	
Model	242.66	11	22.06	58.37	< 0.0001	significant
A-Process Pressure	111.78	1	111.78	295.76	< 0.0001	
B-Time of Flow	41	1	41	108.49	< 0.0001	
C-Type of Element	78.23	2	39.12	103.49	< 0.0001	
AB	0.675	1	0.675	1.79	0.1926	
AC	6.1	2	3.05	8.07	0.0018	
BC	2.3	2	1.15	3.05	0.064	
A^2	0.0541	1	0.0541	0.1433	0.708	
B^2	2.56	1	2.56	6.78	0.0148	
Residual	10.2	27	0.378			
Lack of Fit	7.12	15	0.4749	1.85	0.1443	
Pure Error	3.08	12	0.2568			
Cor Total	252.86	38				

$$Energy\ Released\ (Slit\ venturi) = 10.77 - 2.80A + 0.36B - 0.032AB - 0.20A^2 - 0.0016B^2 \quad (4.4a)$$

$$Energy\ Released\ (Orifice) = 4.36 - 1.23A + 0.34B - 0.032AB - 0.20A^2 - 0.0016B^2 \quad (4.4b)$$

$$Energy\ Released\ (Elliptical\ venturi) = 1.04 - 0.37A + 0.31B - 0.032AB - 0.20A^2 - 0.0016B^2 \quad (4.4c)$$

4.4.5 Numerical optimisation and validation of the CCD model used for the optimization of hydrodynamic cavitation reactor

The operational conditions of the hydrodynamic cavitation system were optimized to maximize the volume flow rate, energy release and total phenolic content while minimizing the cavitation number. For processes involving multiple responses,

the desirability function approach is commonly used for optimization. The optimal operational conditions for the hydrodynamic cavitation reactor were identified using the numerical optimization feature of Design Expert 12 software.

Table 4.8 Optimum criteria of response variables obtained from desirability analysis

Sl. No.	Response	Unit	Desirability	Optimum level	Low level	High level
1	Cavitation number	Dimensionless quantity	In range	0.4	0.15	0.4
2	Volume flow rate	L/h	Maximise	19.8415	3.5	24.3
3	Total phenolic content	mgGAE/ml	Maximise	321.007	307.8	321.87
4	Energy released	J/ml	Maximise	8.24001	0.8	10.676

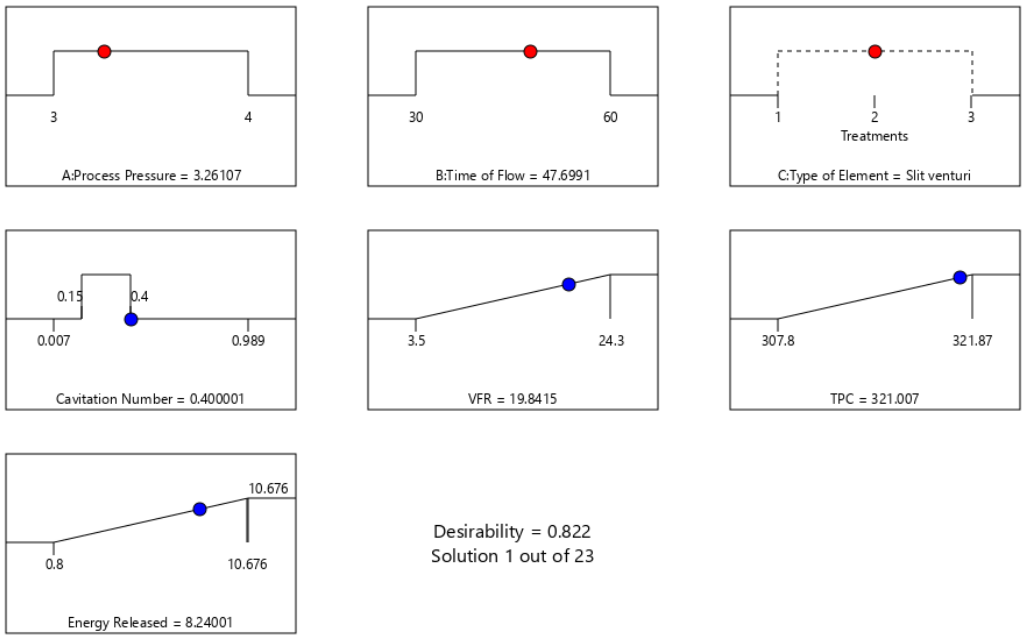

Fig. 4.5 Desirability ramps for numerical optimisation

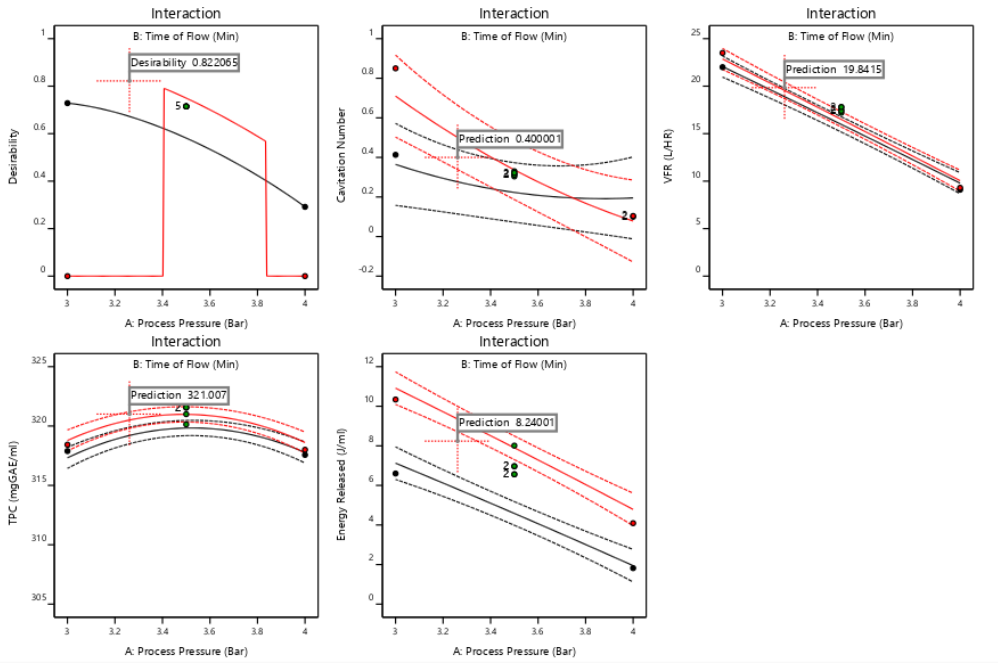

Fig. 4.6 Desirability interaction graphs

The conditions and results of the optimization are detailed in Table 4.8. This feature combines individual desirability values into a single metric, aiming for the highest desirability score, which ranges from 0 to 1. Target and in-range criteria were employed as predictors for the optimization and the desirability ramps plot for the numerical optimization is shown in Figure 4.5.

From the desirability analysis, it was found that the optimum experimental conditions for hydrodynamic cavitation were obtained for the treatment in slit venturi with process pressure of 3.26107 bar and time of flow of 47.6991 minutes. The dependent variables such as cavitation number, VFR, TPC and energy released were recorded as 0.4, 19.8415 L/h, 321.007 mgGAE/ml and 8.24001 J/ml respectively (Table 4.3) at the optimum operating conditions with a desirability of 0.822 as may be seen from the desirability ramps.

4.5 CHARACTERIZATION OF ACCELEARTED AGED COCOA MUCILAGE WINE IN COMPARISON WITH FRESH AND AGED WINE

4.5.1 Total phenolic content

The values for TPC in the case of untreated wine, conventionally aged wine, and HC-treated wine were obtained as 258±0.2 mgGAE/ml, 285±0.21 mgGAE/ml, and 324±0.25 mgGAE/ml respectively (Fig 4.7). It is therefore clear that HC treatment has an influence in increasing the TPC of wine.

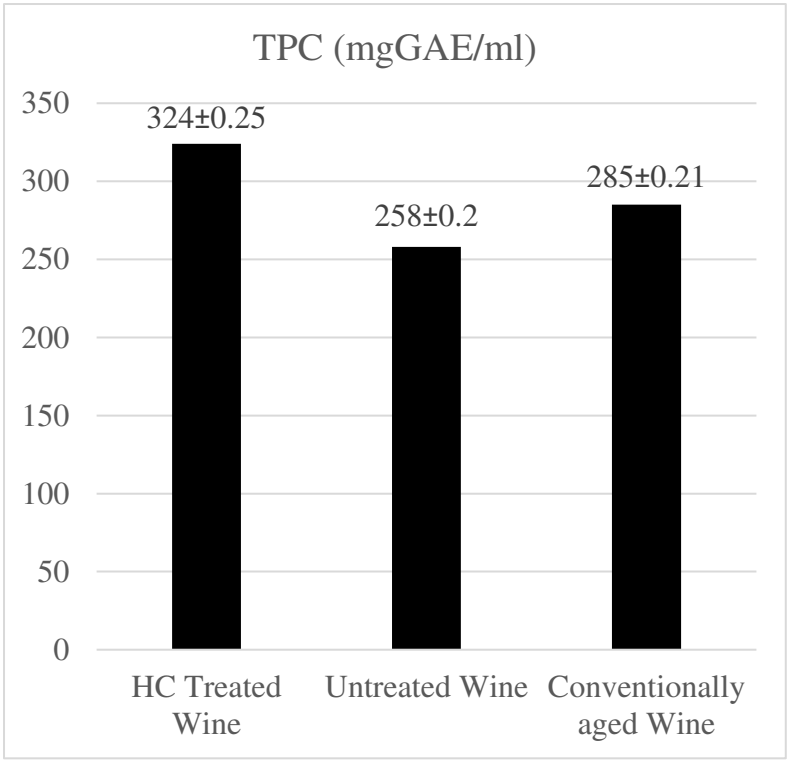

Fig. 4.7 Total phenolic content of 3 wine samples

Since the cavitation impact causes the cells to release phenolic compounds during the coalescence process, total phenols increased as the HC treatment dose increased. According to recent research, phenols are bound to proteins, lignin, pectin, and carbohydrates. Phenolic chemicals will be released into the medium as a result of the ability of HC to break down bigger molecules into simpler ones (Albanese *et al*., 2019).

It was found that the phenolic compounds were stable and resistant to degradation during different treatment time and pressure for HC. Additionally, it was

discovered that HC-treated wine had a higher TPC level than conventionally aged wine. This demonstrates that HC is more effective in extracting phenolic chemicals, simulating the characteristics of wine that has been traditionally aged (Kochadai *et al*., 2022). The TPC of aged wines was found to be higher than young wines for always all the wine making procedures (Baiano *et al*., 2015).

4.5.2 Antioxidant activity

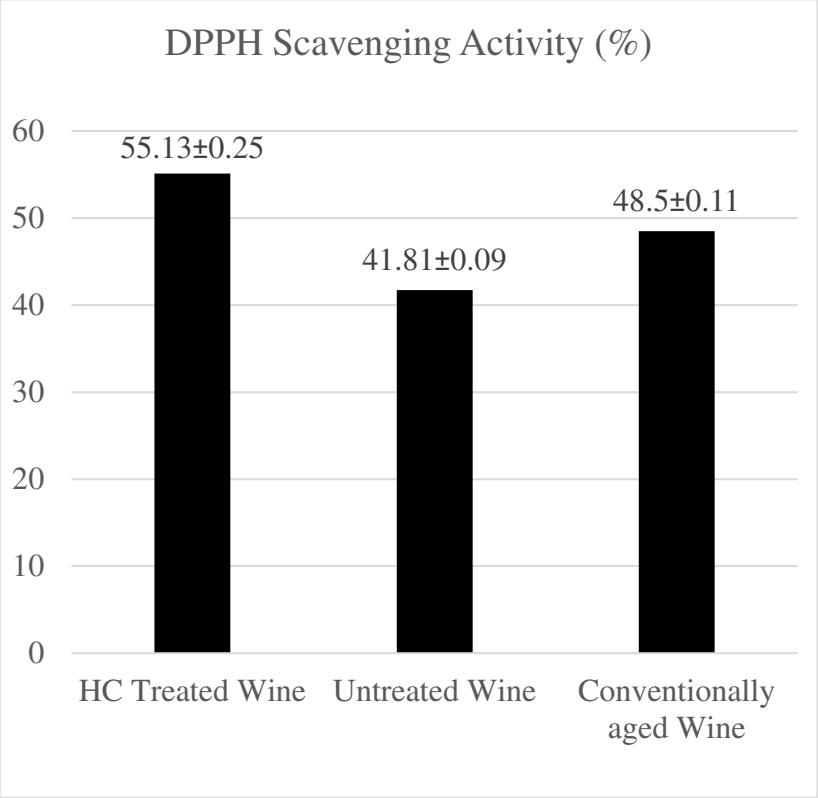

Fig. 4.8 Antioxidant (DPPH) scavenging activity of 3 wine samples

The values of DPPH scavenging activity for untreated wine, conventionally aged wine and HC treated wine were found to be 41.81±0.09, 48.5 ± 0.11 and 55.13 ± 0.25% respectively. Therefore, it is clear that HC treatment has an influence in increasing the antioxidant activity of wine. Antioxidant activity of the residues is correlated with the bioactive compounds of the mucilage. Antioxidant activity showed a strong positive correlation with the procyanidins and other phenols (Llerena *et al*., 2023). The results of the present study exhibited a similar trend as previously described.

The possible reason for the increase in antioxidant content during the HC treatment might be due to better extractability of antioxidant compounds as there was a small hike in temperature and release of dissolved oxygen into the medium (Patras *et al*., 2009).

According to the authors, the release of bound antioxidants including phenols and ascorbic acid is what caused the rise in antioxidant content observed with ultrasonic therapy (Nadeem et al., 2018). Similar to this, blueberry wine treated with mild ultrasonication increased anti-ABTS+ levels (Li *et al*., 2020).

Similar results were observed in HC-treated orange juice (Katariya et al., 2020) and ultrasound assisted (US) accelerated aging in red wine and US treatment, the oxygen concentration significantly decreased to the values close to their controls when the intensities of HC and US increased (Del Fresno *et al*., 2018). According to Nadeem *et al*., (2018), ultrasonic therapy increased antioxidant content, which the authors believe is due to the release of bound antioxidants such as phenols and ascorbic acid.

A study by Canas *et al*., (2008) found that brandies aged in chestnut hardwood barrels demonstrated higher antioxidant activity, with results obtained under laboratory conditions indicating their superior quality. Antioxidant activity and total phenolic compound concentration were shown to be significantly correlated. strong relationships between antioxidant activity and the amounts of gallic, ellagic, and vanillic acids were found, suggesting that these substances can significantly boost the brandies' overall antioxidant capacity. Therefore, the abundance of gallic, ellagic, and vanillic acids in the brandies aged in chestnut wood may contribute to their greater antioxidant activity. Studies that demonstrate the potent antiradical properties of gallic and ellagic acids, even at extremely low concentrations, add evidence to this theory.

4.5.3 Vitamin C

The vitamin C content in the wine exhibited a similar trend to that of total phenols. Compared to untreated wine, the vitamin C content increased in both of conventionally aged wine and HC treated wine. The vitamin C levels for untreated, conventionally aged and HC-treated wines were 0.016±0.002, 0.058±0.002, and 0.252±0.002 respectively.

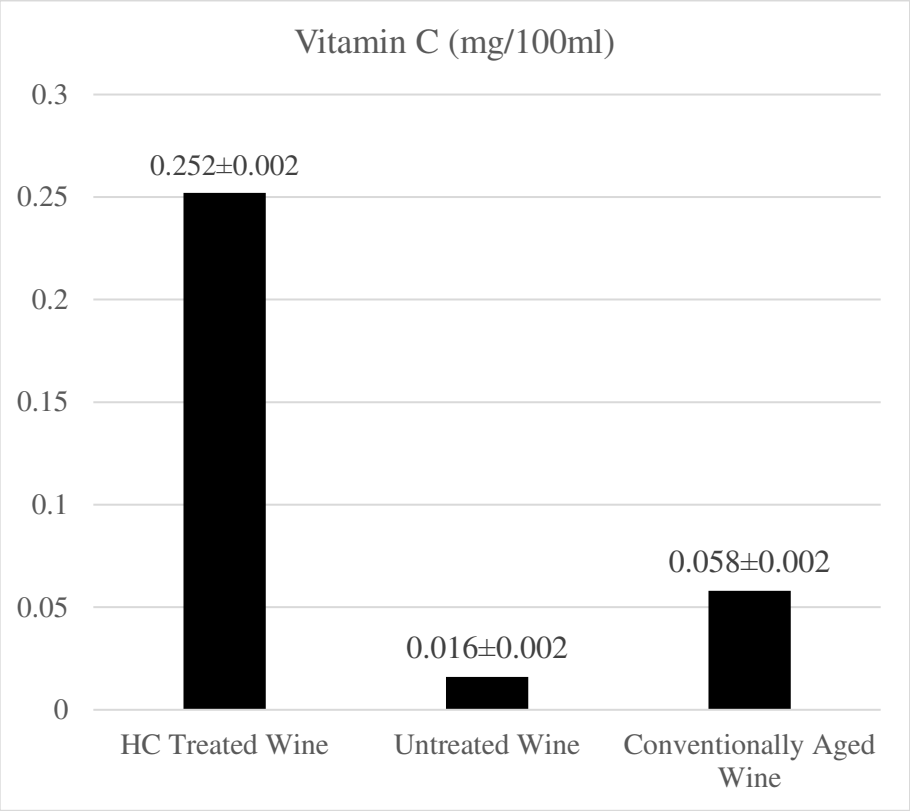

Fig. 4.9 Vitamin C content of 3 wine samples

HC treated sample showed the highest value for vitamin C compared to other two wine samples. This could be as a result of the cavitation effect, which enhanced mass transfer, improved solvent penetration, and disrupted the bond between the vitamins and their coenzymes, allowing the free form of vitamins to be released. (Oladejo *et al*., 2017). Vitamin C in its free state has higher bioavailability than vitamins that leave the food matrix in chemically bound forms, which have poorer absorption efficiency (Panda & Manickam, 2019; Santos *et al*., 2018).

The high retention of vitamin C could be attributed to the removal of dissolved oxygen caused by the cavitation effect, which may have accelerated the degradation of active compounds (Tiwari *et al*., 2009).

The slight increase in vitamin C content during the early stages of conventional wine aging may be due to the release of bound ascorbic acid from compounds in the wine or initial stabilization under controlled conditions. However, this increase is short-lived, as vitamin C levels generally decrease over time due to oxidative degradation (Cendrowski *et al*., 2021). Furthermore, studies have indicated that during the aging

process, wine variants experience a substantial loss of L-ascorbic acid, with reductions ranging from approximately 26% to 42% compared to pre-fermentation levels (Evers *et al*., 2021).

These findings align with the results of the present study, indicating that hydrodynamic cavitation under controlled treatment conditions can effectively enhance phenolic and antioxidant properties, including ascorbic acid content.

4.5.4 Reducing sugar

The reducing sugar content for untreated, aged and HC-treated wine was found to be 21.42%, 24.59% and 22.89% respectively. An increase in reducing sugar levels was observed with HC treatment. The initial rise in reducing sugars can be attributed to the enhanced cavitation effect caused by high pressure, leading to the violent collapse of molecules.

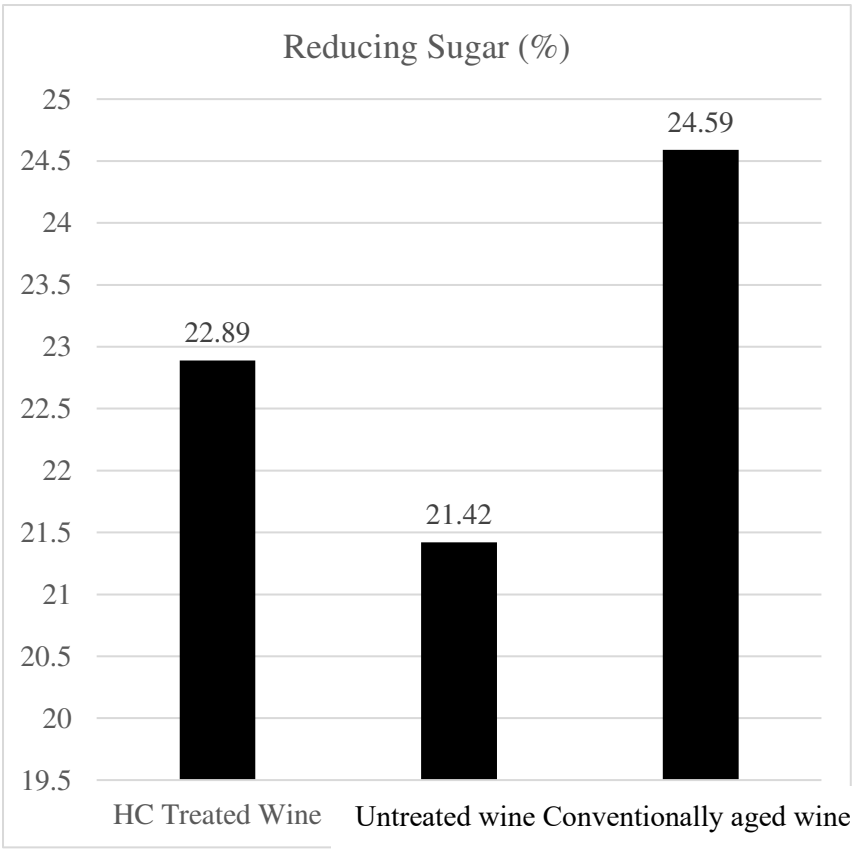

Fig. 4.10 Reducing sugar content of 3 wine samples

Additionally, the smaller diameters in the cavitation reactors generate higher shear forces, resulting in intense pressure, increased turbulence frequency, elevated collapse pressure and improved mass transfer (Arya *et al*., 2020; Joshi & Gogate, 2019). The increase in reducing sugar content is further explained by the formation of multiple hotspots during cavitation, which break glycosidic bonds. These findings are consistent with the results reported by Jiao *et al*., (2020).

4.5.5 pH

The pH values for untreated wine, conventionally aged wine and HC-treated wine were recorded as 3.66, 3.64 and 3.24 respectively. There was no significant difference in pH between untreated and treated wines, regardless of the treatment duration. Despite minor variations, the wine's pH remained below 4, which is ideal for low-alcohol wines as the acidic environment inhibits the growth of undesirable bacteria (Mutiat *et al*., 2017).

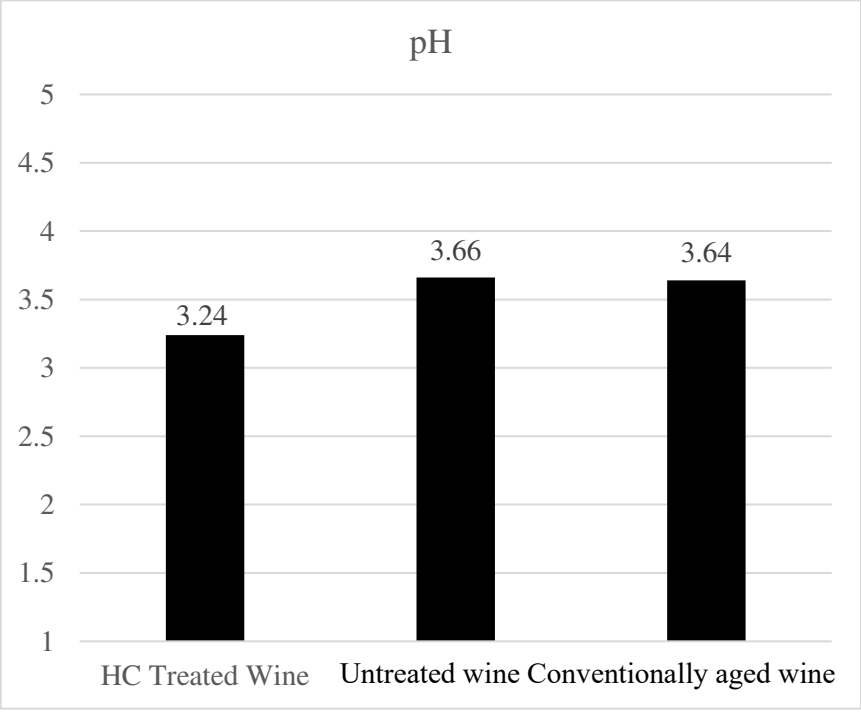

Fig. 4.11 pH values of 3 wine samples

These findings are consistent with earlier research on the impact of HC on orange juice, which found no discernible change in pH or acidity in response to variations in cavitation severity.

Additionally, there were no discernible differences in pH or acidity between the control and HC treated samples when hydrodynamic cavitation was used for processing of tomato juice (Vigneshwaran *et al*., 2022). Similarly, there was no apparent distinction in pH or overall acidity between giant squid protein solutions and blueberry juice after ultrasound processing (Higuera-Barraza *et al*., 2017). Li *et al*., (2020) also discovered that the pH of the soy protein isolate was not significantly altered by either HC or ultrasonic. Similar outcomes were noted by Adekunte *et al*., (2010) while processing tomato juice by sonication, suggesting that the pH and acidity changes were negligible irrespective of the treatment amplitude level and duration.

4.5.6 Titrable acidity

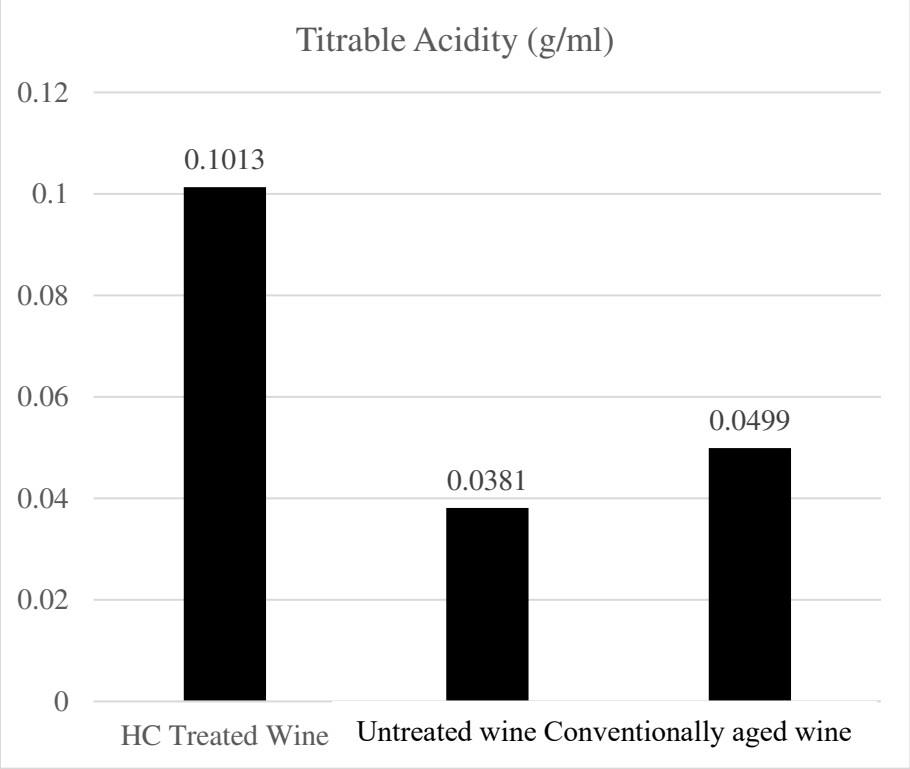

Fig. 4.12 Titrable acidity content of 3 wine samples

Titrable acidity values for untreated, conventionally aged and HC treated wine were obtained as 0.0381, 0.0499 and 0.1013 g/ml (tartaric acid). Titrable acidity of conventionally aged wine is higher than untreated wine. Similarly, titrable acidity of HC treated wine were found to be higher than that of other two samples. The increase

in the titrable acidity is due to the decrease in pH during the hydrodynamic cavitation treatments.

Both wines showed a progressive drop in pH and an increase in titratable acidity as they aged. This could be because when fruit wines are aged, the oxidation of sugar molecules into organic acid raised their titratable acidity and lowered their pH level (Adiyaman *et al*., 2019).

According to a study on peanut milk, sonicating it for ten minutes significantly increased its titrable acidity (Salve, Pegu, and Arya 2019). The rise in titrable acidity is supported by the similar declining trend of pH.

4.5.7 TSS

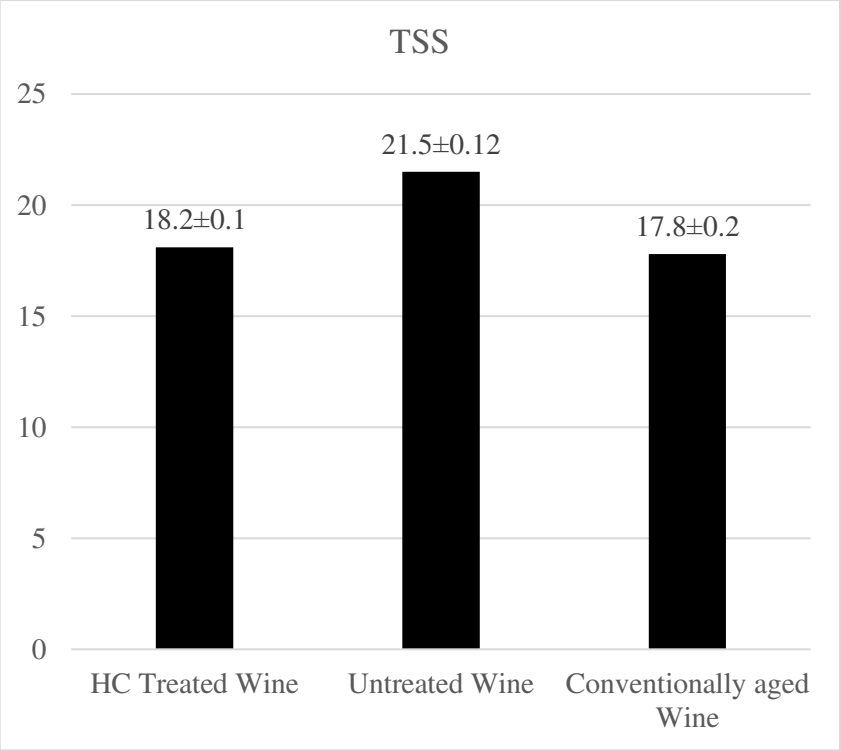

Fig. 4.13 TSS content of 3 wine samples

TSS for untreated wine, conventionally aged wine and HC treated wine were found to be 21.3±0.15, 17.3±0.2 and 18.2±0.1 respectively. TSS of wine decreased with conventional aging and HC treatment. The TSS of the untreated wine reduced due to HC treatment as the treatment period increased. This is because when the solid particles are closer to the cavitation bubbles, they form symmetric and asymmetric impurities

that break down the suspended solids in the medium. In the same way, Katariya *et al*., (2020) found that orange juice treated in HC significantly decreased TSS. This outcome was in line with sugarcane juice treated with HC, where the TSS was considerably lowered from 20 °Brix to 12 °Brix as a result of an increase in inlet pressure. According to Gani *et al*., (2016), treating strawberries with higher ultrasonic intensity results in lower TSS.

As aging progressed, the TSS content of the fruit wines decreased further. This decreasing trend in TSS aligns with previous findings. For example, a study conducted by Bhatane and Pawar (2013), reported a reduction in TSS content in sapota wine during aging, while Maragatham and Panneerselvam (2011) observed a decline in the TSS content of papaya wine from 12.14 to 9.36 °Brix as aging progressed.

4.5.8 Colour

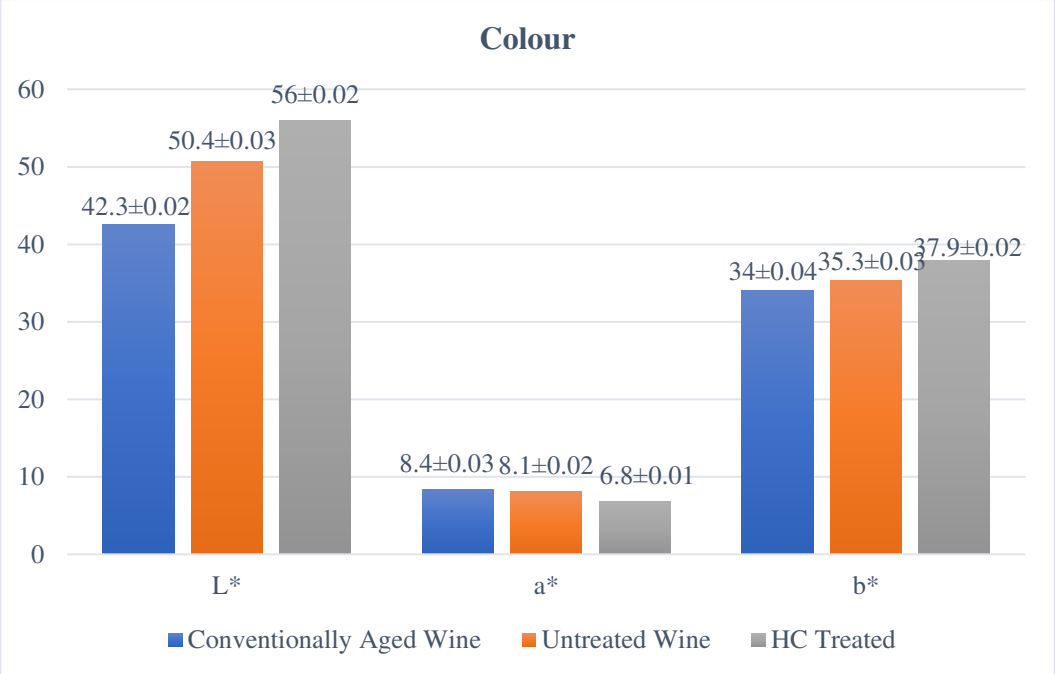

Fig. 4.14 Colour values (L*, a* and b*) of 3 wine samples

The color of the wine is one crucial factor that influences consumer preference. L* & b* values showed an increase and a* value decreased as the wine ages. The increase in L* value as aging progress, indicates that the wine becomes lighter in colour. The cause for the increased lightness in wine would be the slow loss of colours that

occurs during aging and filtration (Rivas et al., 2006). The L* value rose. This is because heat and pressure work together to create shear stress through cavitation, which triggers the browning-causing endogenous enzymes found in the wine. Similarly, Sun *et al*., (2015) found that apple juice treated with ultrasound had a higher browning index than untreated juice. This outcome is consistent with the earlier research by Carvalho *et al*., (2015) on the aging of Madeira wines with oak chips, which found that aging raised the L* values.

Increase in b* value indicates that yellow colour has significantly imparted as aging progressed (Recamales *et al*., 2006). The yellow hue could be caused by the formation of orange-yellow pigments that come from anthocyanin pigment reactions or the oxidation of substances like flavanols (Picariello *et al*., 2017). Additionally, the a* values tended to move toward the green color as the duration of HC therapy increased becoming more negative (Recamales *et al*., 2006).

4.5.9 Alcohol content

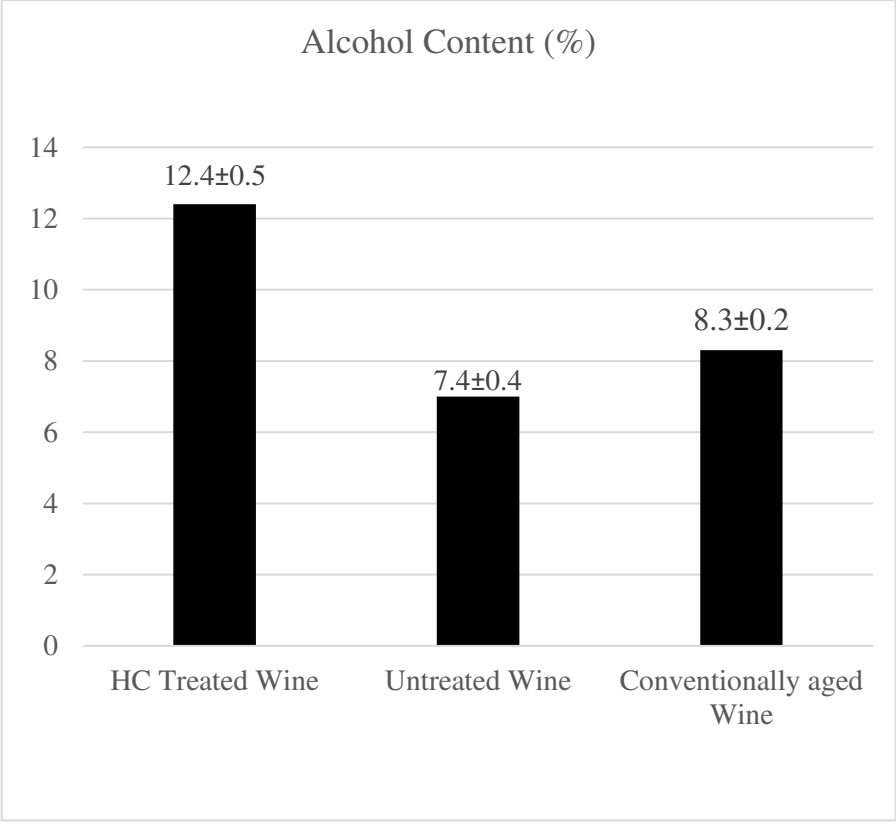

Fig. 4.15 Alcohol content of 3 wine samples

Alcohol content of untreated, conventionally aged and HC treated wine were found to be 7.4±0.4, 8.3±0.2, 12.4±0.5% respectively. Alcohol content increases as aging continues. It is due to the steeped decrease of TSS during aging. This is attributed to high fermentability of wine, due to the availability of high amount of sugar (Thungbeni *et al*., 2020).

HC treated wine contains highest percentage of alcohol. HC increased ethanol yield in US corn. Because HC increases the number of sugars accessible, cavitation causes increases in ethanol output. More soluble glucose equivalents (starch, polysaccharides, oligosaccharides, and glucose monomers) were produced by cavitation, increasing the amount of glucose that can be fermented during Simultaneous Saccharification and Fermentation (SSF). The increase in ethanol output and glucose equivalents is consistent with the findings of Ramirez Cadavid *et al*., (2016) at a commercial ethanol plant that utilizes high energy density hydrodynamic cavitation.

4.5.10 Mineral analysis

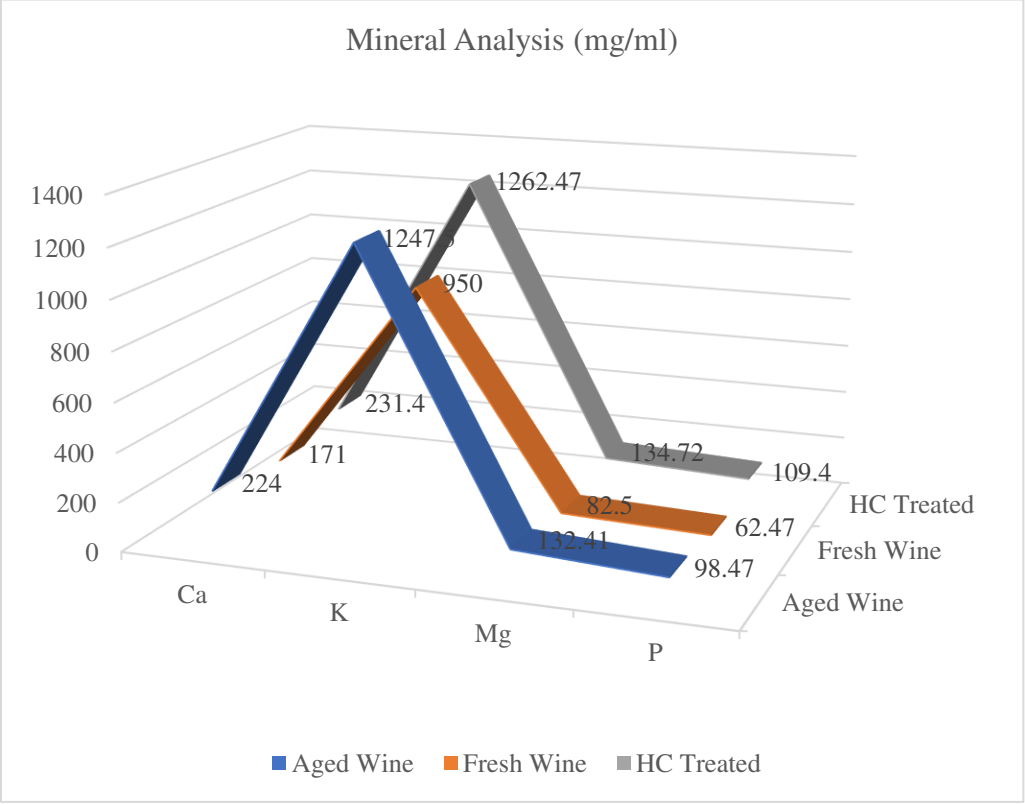

Fig. 4.16 Mineral content of 3 wine samples

All four mineral elements show a significantly positive increase during the aging process in both conventionally aged and accelerated aged samples. Both types of aged samples exhibit higher values compared to the untreated (fresh) cocoa mucilage wine samples.

Among the minerals, potassium displayed the highest value (Soares and Oliveira, 2022). Of the three types of wines, the HC-treated wine exhibited the highest mineral content. Hydrodynamic cavitation enhances the extraction of soluble components, including minerals. The intense cavitation conditions help break down cellular structures, facilitating the release of minerals.

4.5.11 Sensory evaluation

Consumer acceptance plays a vital role in the successful development of a product and in assessing its market value. Sensory analysis, a scientific approach, involves the use of human senses via., sight, smell, taste, touch and hearing in order to evaluate and interpret the characteristics of food products. Based on the mean scores of the sensory parameters from 15 panellists, the best wine was chosen. The mean scores of the sensory panellists are given in Table 4.9 and the results were plotted as a spider web chart (Fig. 4.18) as well as bar chart with grouping of treatments based on LSD test (Fig. 4.17). Sample T4 was given the highest score, followed by T2 and T5. This is because the samples treated with HC shows better results in pH, TSS, TPC, DPPH activity, alcohol content etc., which contributed to the better and desirable flavour.

Table 4.9 Sensory scores of different cocoa mucilage wines

Samples	Aroma	Taste	Appearance	Mouthfeel	After Taste	Overall Acceptability
T1	6.2 ± 1.52^{c}	5.93 ± 1.79^{c}	7.6 ± 1.18^{a}	6.13 ± 1.59^{c}	6.2 ± 1.82^{c}	6.26 ± 1.53^{c}
T2	7.53 ± 0.99^{ab}	7.4 ± 1.12^{ab}	7.0 ± 1.07^{ab}	7.4 ± 1.05^{ab}	7.4 ± 0.83^{ab}	7.53 ± 0.64^{ab}
T3	6.67 ± 1.29^{bc}	6.73 ± 1.39^{bc}	7.06 ± 0.88^{ab}	6.4 ± 1.59^{bc}	6.46 ± 1.4^{bc}	6.87 ± 0.99^{bc}
T4	$\mathbf{7.67\pm1.35^{a}}$	$\mathbf{7.8\pm1.01^{a}}$	$\mathbf{7.13\pm1.24^{ab}}$	$\mathbf{7.46\pm1.59^{a}}$	$\mathbf{7.67\pm1.11^{a}}$	$\mathbf{7.93\pm0.7^{a}}$
T5	6.73 ± 1.39^{abc}	6.67 ± 1.35^{bc}	6.73 ± 0.96^{b}	6.73 ± 1.10^{abc}	6.73 ± 1.1^{abc}	6.87 ± 0.99^{bc}

Note: Different superscripts within the same column indicate significant differences at $p<0.05$

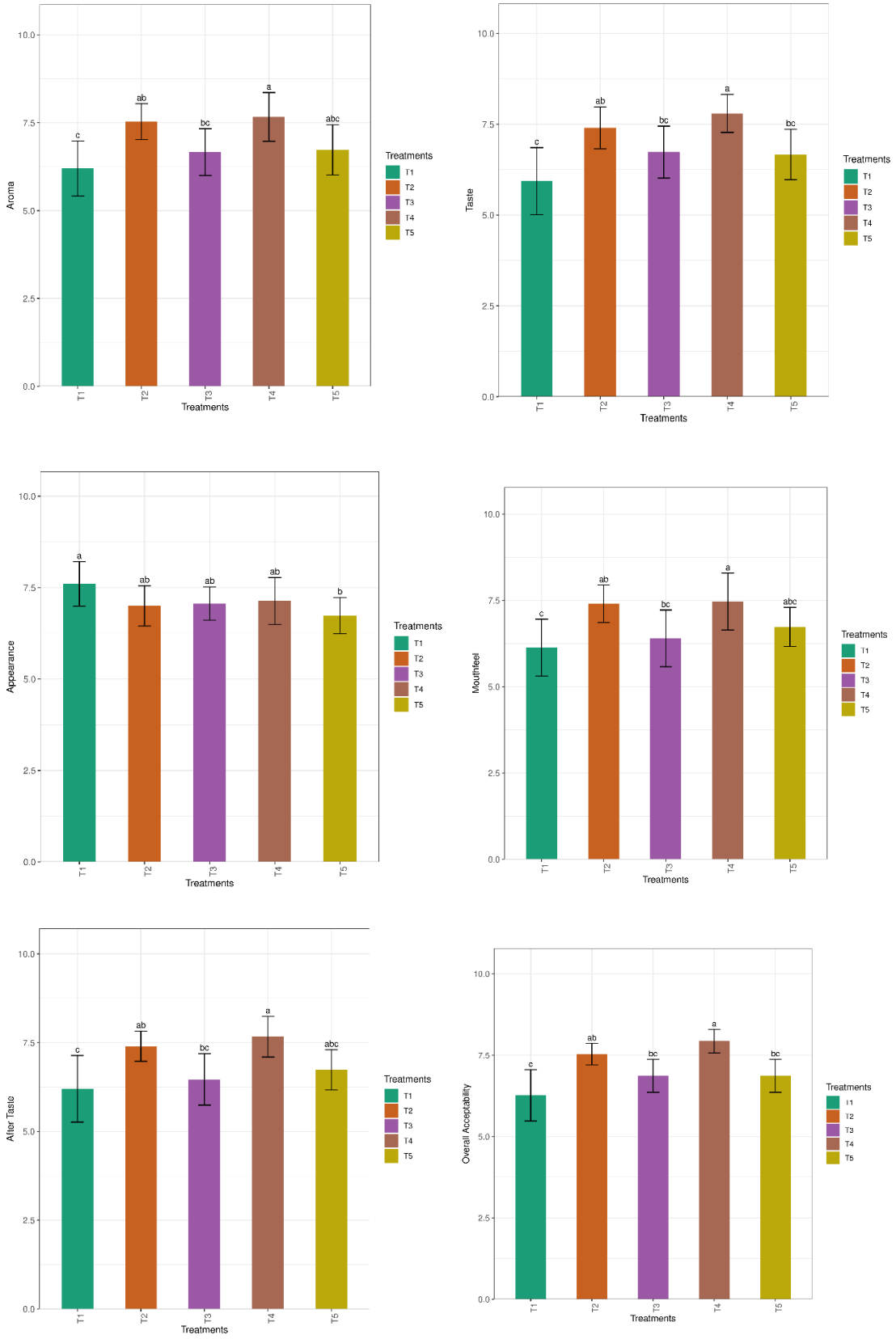

Fig 4.17 Bar chart with grouping based on LSD test

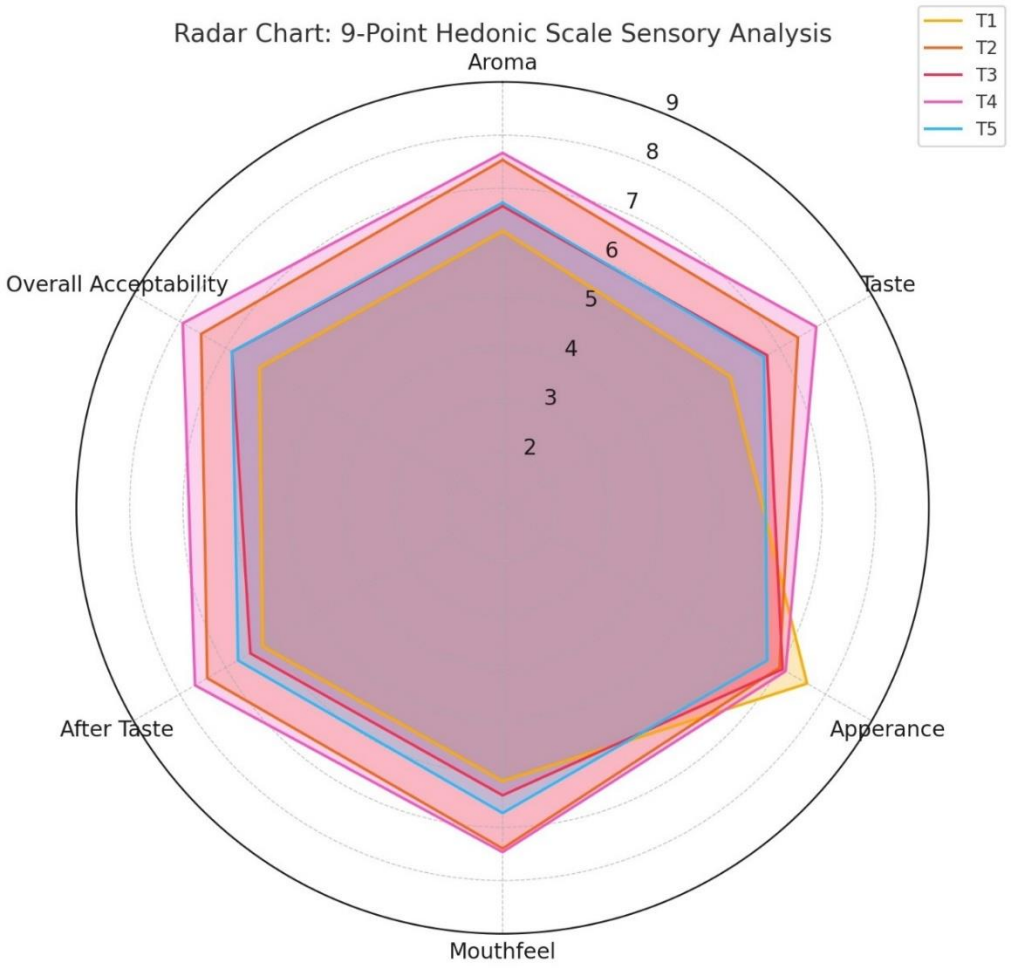

Fig. 4.18 Sensory analysis of different cocoa mucilage wines

4.5.12 Cost estimation

The production cost of one litre of accelerated aged cocoa mucilage wine through HC treatment was estimated to be Rs. 227.105/-. The benefit-cost ratio of 10 year conventionally aged cocoa mucilage wine to the accelerated aged cocoa mucilage wine through HC treatment was calculated as 1.09:1. Detailed computations are tabulated and presented in Appendix A.